第 28 卷第 9 期
2012 年 9 月

无 机 化 学 学 报
CHINESE JOURNAL OF INORGANIC CHEMISTRY

Vol.28 No.9
1985-1996

两个多胺铜配合物的合成,晶体结构以及 DNA 切割活性

文小明 胡 虹 周 红 潘志权*

(武汉工程大学绿色化工过程教育部重点实验室,武汉 430073)

摘要: 本文以配体 *N*,*N*′-二(3-氨丙基)-4-甲氧基苄胺(amba)与 4,4′-联吡啶,铜盐反应合成了两种多胺 Cu(Ⅱ)配合物[Cu(amba)Cl_2] (**1**)和[Cu(4,4′-bipy)(amba)(ClO_4)]ClO_4 (**2**),通过红外光谱、质谱和 X-射线单晶衍射对其结构进行了表征。利用紫外吸收光谱、分子荧光,电化学以及粘度试验研究了配合物与小牛胸腺 DNA(CT-DNA)的相互作用方式。通过紫外吸收光谱得到配合物 **1** 和 **2** 与 DNA 的结合常数 K_b 分别为 1.3×10^4 $mol^{-1}\cdot L$ 和 1.7×10^4 $mol^{-1}\cdot L$, 荧光光谱得到配合物 **1** 和 **2** 的荧光淬灭常数分别为 1.04×10^3 $mol^{-1}\cdot L$ 和 1.81×10^3 $mol^{-1}\cdot L$, 表明了配合物 **1** 和 **2** 与 CT-DNA 结合方式均为静电模式。凝胶电泳实验的结果表明配合物对 pBR322 DNA 的切割均为水解切割。

关键词: 多胺铜配合物; 晶体结构; 结合方式; DNA 切割

中图分类号: O614.121 **文献标识码**: A **文章编号**: 1001-4861(2012)09-1985-12

Synthesis, Crystal Structure, and DNA Cleavage Activity of Two Polyamine Copper(Ⅱ) Complexes

WEN Xiao-Ming HU Hong ZHOU Hong PAN Zhi-Quan*

(*Key Laboratory for Green Chemical Process of Ministry of Education, Wuhan Institute of Technology, Wuhan* 430073, *China*)

Abstract: Two functional polyamine copper(Ⅱ) complexes, [Cu(amba)Cl_2] (**1**) and [Cu(4,4′-bipy)(amba)(ClO_4)]ClO_4 (**2**), have been obtained easily via evaporation of the mixture of *N*,*N*-bis(3-aminopropyl)-4-methoxybenzylamine (amba) and 4,4′-bipy and cupric salts. The complexes were characterized by IR, ES-MS and X-ray single crystal diffraction techniques. The interactions of the complexes with calf thymus DNA (CT-DNA) have been measured by UV-Vis absorption, fluorescent spectroscopy, electrochemical experiment and viscosity experiment. Absorption spectroscopic investigation reveals that the calculated binding constants (K_b) values for the two complexes are 1.3×10^4 $mol^{-1}\cdot L$ for **1** and 1.7×10^4 $mol^{-1}\cdot L$ for **2**, respectively. Fluorescence spectroscopy shows that Stern-Volmer quenching constants of complexes **1** and **2** are 1.04×10^3 $mol^{-1}\cdot L$ and 1.81×10^3 $mol^{-1}\cdot L$, respectively. The results indicate that the binding modes of the two complexes interact with DNA may be not intercalative modes but electrostatic modes. Moreover, the higher constant value of **2** shows the interaction of **2** with DNA is stronger than that of **1**. The agarose gel electrophoresis studies reveal that both the complexes cleave pBR322 DNA via a hydrolytic pathway. CCDC: 867405, **1**; 867404, **2**.

Key words: polyamine copper complex; crystal structure; binding bind; DNA cleavage

Polyamines have drawn considerable attention in the past decade due to their structural and the diversity of coordination modes. So far, many efforts have been made to synthesize a variety of polyamines[1]. At the same time, many of metal polyamine complexes were obtained for mimicking the active sites of metal-

收稿日期:2012-03-05。收修改稿日期:2012-04-26。

国家科学自然基金(No.20871097,20971102);湖北省中青年人才项目(No.T200802)资助项目。

*通讯联系人。E-mail:zhiqpan@163.com

loproteins and metalloenzymes, and studying the relationship between their structures and properties[2]. On the other hand, polyamines can be used for constructing multifunctional materials, such as magnetism, optic, catalysis, microporosity, molecular sorption and recognition[3-8]. Furthermore, the artificial polyamine complexes are also applied to facilitate DNA transfection of cellular fission, biosynthetic enzymes and cure of neurological illness[9].

It is well known that DNA is very sensitive to oxidative cleavage, so many studies on mimicking enzyme have been focused on molecules capable of cleaving DNA oxidatively[10]. Most of these molecules can just induce effective oxidative cleavage of DNA in the presence of UV light, a reducing agent or an additive, such as H_2O_2[10-11]. However, notwithstanding their high efficiency and versatility, oxidative cleavage products are not readily manipulative to further enzymatic controlling, and thus have limited use in molecular biology. However, hydrolytic cleaving agents do not have these faults. The synthetic metallohydrolases follow a mechanistic pathway closed to the phosphate-diester bonds acting on the nucleosides which leads to the formation of fragments like endonucleases [12]. So study on metallohydrolases capable of mimicking the function of these endonucleases has been paid more and more attention. Many transition metal complexes including the polyamine ligands actually have exhibited the ability of hydrolytic cleavage of DNA[13]. However, most of these ligands used were confined to macrocyclic polyamines and those with an ethoxyl pendent[14] and few of the former research works have been concentrated on tripodal polyamines bearing a phenoxide pod. The tripods should have some advantages over the macrocyclic polyamines because the tripodal ligands often construct a trigonal-dipyramidal environment around the captured metal ion, leaving the fifth coordination point vacant, which facilitates the ligation of free solvent molecular or the substrates in catalytic process, while, comparatively, the macrocyclic ligands tends to be more rigid in coordination modes. Tang reported a zinc(Ⅱ) 2-[bis(2-aminoethyl) amino]ethanol, its hydrolysis of esters are at least as good as macrocyclic polyamines[15]. Considering that the aryl-groups can insert into base-pairs of DNA via π-π intereaction and alkyloxide can form hydrogen bonds with base-pairs, we designed and synthesized the 4-methoxybenzyl functional N^1-(3-aminopropyl) propane-1,3-diamine to serve as ligand to construct polyamine complexes. Herein, we report the synthesis, crystal structure and DNA cleavage activity of two copper(Ⅱ) complexes of amba. Although the structures of ligand and complexes are simple than the macrocyclic polyamine ligand and their complexes, present work shows that these simple Cu(Ⅱ) complexes can also be good models of phosphate-ester hydrolytic enzymes.

1 Experimental

1.1 Materials and characteristication

All solvents and chemicals were of analytical grade and used as received, except methanol that was purified to absolute one by general method. *N*,*N*-bis(3-aminopropyl)-4-methoxybenzyl ammonium chloride (amba·3HCl) was prepared according to literature[16].

CT-DNA were obtained from Alfa Aesar and used as received. Tris (hydroxymethyl)amino-methane (Tris), bromophenol blue, ethidium bromide (EB), agarose gel and plasmid pBR322 DNA were purchased from TOYOBO Co. The buffer solutions were prepared with double-distilled water. TAE buffer: 24.2 g tris base, 5.7 mL acetic acid and 3.72 g EDTA in 100 mL water, pH=8. BSE solution: 0.25% bromophenol blue and 40% (*W*/*W*) saccharose. EB solution: ethidium bromide 0.1 g in 100 mL double-distilled water.

Elemental analyses were performed on a Vario EL III CHNOS elemental analyzer (Elementar, Germany). IR spectra were recorded on a vector 22 FI-IR spectrophotometer using KBr disc. Electronic spectra were performed on an UV-2450 spectrophotometer to observe the absorption spectra in the 200~500 nm range. Electrospray mass spectra were determined on a Finnigan LCQ ES-MS mass spectrograph using methanol as the mobile phase with a sample concentration of about 1.0 mmol·L^{-3}. The diluted solution was electrosprayed at a flow rate of 5×10^{-6} dm^3·min^{-1} with a needle voltage of +4.5 kV. The temperature of

the heated capillary in the interface was 200 ℃ and a fuse silica sprayer was used.

1.2 Synthesis of complex [Cu(amba)Cl_2] (1)

Amba·3HCl (0.126 g, 0.5 mmol) in 15 mL water was adjusted to pH=7 with NaOH solution. $CuCl_2 \cdot H_2O$ (0.067 g, 0.5 mmol) in 10 mL methanol was added slowly to the resulting solution. After stirring at ambient temperature for about 10 h and slowly evaporating at room temperature over 2 d, blue single crystals suitable for X-ray diffraction were obtained. Yield: 0.22 g (62%). Anal. Calcd. for $C_{14}H_{25}ON_3Cl_2Cu$ (%): C 43.6, H 6.5, N 10.9. Found (%): C 43.4, H 6.5, N 10.9. IR (KBr, ν/cm^{-1}): 3 236, 3 118 (N-H), 1 248, 1 031 (C-O), 817, 751, 704(C-H) (phenyl).

1.3 Synthesis of complex [Cu(4,4′-bipy)(amba)(ClO_4)]ClO_4 (2)

Amba·3HCl (0.126 g, 0.5 mmol) in 15 mL water was adjusted to pH=7 with NaOH solution. The resulting solution was extracted by dichloromethane. After separated the water, the solution was dried with anhydrous sodium sulfate and solvent was removed under reduced pressure. The remainder was dissolved in 10 mL anhydrous methanol, and added to $Cu(ClO_4)_2 \cdot 6H_2O$ (0.185 g, 0.5 mmol) solution (10 mL) of methanol. After stirring at room temperature for a moment, 4,4′-bipyridine (0.078 g, 0.5 mmol) was added to the solution. The suspension was filtered. Insoluble product was dissolved in water. Blue single crystals suitable for X-ray investigation were obtained by slow evaporation at room temperature over 2 d. Yield: 0.22 g (62%). Anal. Calcd. for $C_{24}H_{33}O_9N_5Cl_2Cu$ (%): C 41.1, H 4.7, N 10. Found (%): C 41.2, H 4.7, N 9.9. IR (KBr, ν/cm^{-1}): 3 256, 3 315 (N-H), 1 081, 624 (ClO_4^{-1}), 1 247, 1 032 (C-O).

1.4 DNA-binding and cleavage experiments

CT-DNA (20 mg) was dissolved in 100 ml of Tris-HCl buffer (50 mmol·L^{-1} Tris-HCl, 50 mmol·L^{-1} NaCl, pH=7.4) and keep at 4 ℃ for less than 4 d. A_{260}, A_{280} of the above solution were determined on UV-Vis spectrophotometer and A_{260}/A_{280} should be between the ranges of 1.8~2.0. The DNA concentration was determined via absorption spectroscopy using the molar absorption coefficient of 6 600 mol^{-1}·L·cm^{-1} (260 nm) for CT-DNA[14].

The copper complexes were dissolved in double-distilled water at a concentration of 5.0×10^{-5} mol·L^{-1}. The UV absorption titrations were performed by keeping a concentration of the complex while varying the DNA concentration. Complex-DNA solutions allowed to incubate for 30 min before measurements were made. The intrinsic binding constant K_b was calculated according to Eq. (**1**) [15].

$$\frac{c_{DNA}}{|\varepsilon_a-\varepsilon_f|}=\frac{c_{DNA}}{|\varepsilon_b-\varepsilon_f|}+\frac{1}{K_b(|\varepsilon_a-\varepsilon_f|)} \quad (\mathbf{1})$$

ε_a, ε_f and ε_b are the molar extinction coefficients of the solution containing both complex and DNA, free complex, and the complex bound to DNA, respectively.

Fluorescence quenching experiments were performed by adding the solution of complex (1.5 μL) into EB-bound CT-DNA solution (1.5 μL) at different concentrations (from 0 to 200 μmol·L^{-1}). All samples were excited at 520 nm, and emission was recorded at 530~700 nm.

Cyclic voltammograms was measured in DMF, using tetrabutyl ammonium perchlorate (TBAP) as supporting electrolyte. Scanning scope was in the range of −1.1~−0.4 V, and scanning rate was 100 mV·s^{-1}. $E_{1/2}=(E_{pa}+E_{pc})/2$, where E_{pc} is cathodic peak potential, E_{pa} is anodic peak potential[15].

Viscosity measurements were carried out using a capillary viscometer at a constant temperature. Data are presented as $(F/F_0)^{1/3}$ versus molar ratio of complex to DNA[14], where F and F_0 are the viscosity of DNA bonding with complex and viscosity of DNA, respectively.

The cleavage of pBR322 DNA by the complex was examined by gel electrophoresis experiments. Negative supercoiled pBR322 DNA (0.5 μL, 0.5 μg·μL^{-1}) was treated with different concentrations of complex (1 μL) in Tris-HCl buffer (1 μL). After mixing, the mixtures were incubated at 37 ℃ for 3 h. The reactions were quenched by the addition of sterile solution (1 μL, 0.25% bromophenol blue and 40% ((*W*/*W*) sucrose). The samples were then analyzed by electrophoresis for about 1 h at 100 V on agarose gel in TAE buffer (40 mmol·L^{-1} Tris-base, 40 mmol·L^{-1} acetic acid and 1

mmol·L^{-1} EDTA, pH=7.4). The gel was stained with EB (1 μg·μL^{-1}) after electrophoresis and then photographed.

1.5 Determination of the crystal structure

Diffraction intensity data were collected on a Bruker Smart Apex CCD area-detector diffractometer at 293 K using graphite monochromatic mo *Kα* radiation (*λ*=0.071 073 nm). Cell refinement and data reduction were performed by SMART and SAINT programs[17]. The structures were solved by direct methods (Bruker SHELXTL) using all unique data[18]. The non-H atoms in the structures were treated as anisotropic. Hydrogen atoms were located geometrically and refined in a riding mode.

CCDC: 867405, **1**; 867404, **2**.

2 Results and discussion

2.1 Synthesis and characterization

The complexes were obtained by the reaction amba in the presence of $CuCl_2·6H_2O$ and $Cu(ClO_4)_2·6H_2O$ in methanol solution. When amba·3HCl served as starting material, complex **1** was formed with chemical formula [Cu(amba)Cl_2], while amba served as starting material, complex **2** was formed with chemical formula [Cu(amba)(4,4′-bipy)ClO_4]ClO_4, which were showed by elemental analyses and X-ray structure determinations. These results indicated that the coordinated small molecules can leave loose of the metals easily. In IR spectra of the complexes, strong bands are found at 1 247, 1 032 cm^{-1} for complex **1** and 1 248, 1 031 cm^{-1} for **2**, which can be attributed to C-O stretching vibration peak. Also, N-H stretching vibration peak are observed at 3 256, 3 315 cm^{-1} for complex **1** and 3 236, 3 118 cm^{-1} for **2**, respectively. Based the above two points, it means that the target complexes have been synthesized.

2.2 Electrospray mass spectra

The ES-MS spectra of complex **1** in methanol solution is dominated by a peak at *m/z* 349.08, corresponding to [Cu(amba)Cl]$^+$ ($C_{14}H_{25}ClCuN_3O$, Calcd. 349.10), which indicates that coordinated Cl ion can leave from the metal ion easily. For complex **2**, the peak at *m/z* 933.25 can be designated the solvated molecule for six-coordinate copper amine ion {[Cu(4,4′-bipy)$_2$(amba)(ClO_4)]·3EtOH·MeOH·2H_2O}$^+$ ($C_{41}H_{67}ClCuN_7O_{11}$, Calcd. 933.03), which is dominant confirming that Cu^{2+} can form mixed coordinated complex, with the ligand, 4,4′-bipy, and perchlorate ion. The ES-MS spectrum shows that complex **1** is not stable enough in methanol solution.

2.3 Structure description

2.3.1 Crystal structure of [Cu(amba)Cl_2] (**1**)

Unsymmetrical ellipsoid structural unit of complex **1** is given in Fig.1, together with the atom numbering scheme. The crystallographic data and details about the data collection are presented in Table 1, and selected bond lengths and angles relevant to the copper(Ⅱ) coordination polyhedron are listed in Table 2. Hydrogen bond lengths and angles relevant to the two complexs are listed in Table 3.

The complex **1** contains a mononuclear unit [Cu(amba)Cl_2], and the copper(Ⅱ) was five-coordinated displaying a square-pyramidal configuration. In the structure, the copper atom is coordinated with three N

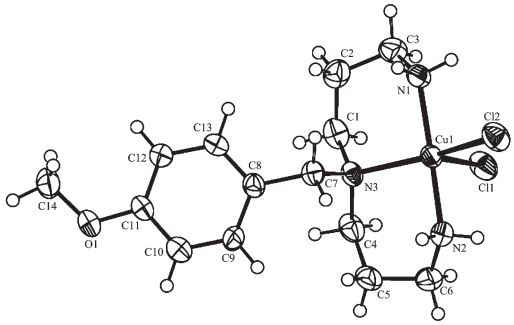

Fig.1 Unsymmetrical ellipsoid structural unit of complex **1** with 50% probability level

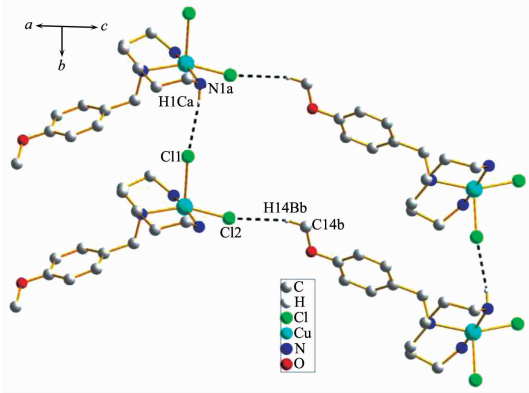

Symmetry codes: a: *x*, −1+*y*, *z*; b: −0.5+*x*, 2.5−*y*, 0.5+*z*

Fig.2 View of the hydrogen bonding interactions of complex **1**

Table 1　Crystal data and structure refinement for complex 1 and 2

	1	2
Empirical formula	$C_{14}H_{25}Cl_2CuN_3O$	$C_{24}H_{33}Cl_2CuN_5O_9$
Formula weight	385.81	699.99
System	Monoclinic	Monoclinic
Space group	$P2_1/n$	$C2/c$
a / nm	1.495 0(2)	3.190 2(3)
b / nm	0.675 75(11)	1.199 36(10)
c / nm	1.838 0(3)	1.523 79(13)
β / (°)	111.154(2)	100.600(1)
Volume / nm^3	1.731 7(5)	5.730 8(8)
Z	4	8
D_c / (g·cm^{-3})	1.48	1.553
μ(Mo $K\alpha$) / nm	1.572	1.008
F(000)	804	2 776
Size / mm	0.22×0.24×0.30	0.22×0.24×0.28
T / K	291	291
Mo $K\alpha$ radiation / nm^3	0.071 073	0.071 073
θ range / (°)	2.2~26.0	2.2~26.0
N_{ref}, N_{par}	3 404, 191	5 612, 371
Tot., uniq. data R_{int}	9 269, 3 404, 0.025	16 318, 5 612, 0.045
Observed data (I>2.0σ(I))	2 829	4 389
R, wR_2, S	0.033 2, 0.088 4, 1.08	0.056 3, 0.142 9, 1.08
Max. and Av. Shift / error	0.00, 0.00	0.00, 0.00

Table 2　Selected bond lengths (nm) and bond angles (°) for complex 1 and 2

			1		
Cu1-Cl1	0.252 64(9)	Cu1-N1	0.198 1(2)	Cu1-N3	0.213 9(2)
Cu1-Cl2	0.237 33(9)	Cu1-N2	0.199 2(2)		
Cl1-Cu1-Cl	107.63(3)	Cl2-Cu1-N1	85.49(7)	N1-Cu1-N3	92.98(9)
Cl1-Cu1-N1	98.76(6)	Cl2-Cu1-N2	84.70(8)	N2-Cu1-N3	91.46(9)
Cl1-Cu1-N2	94.56(6)	Cl2-Cu1-N3	155.52(6)		
Cl1-Cu1-N3	96.77(6)	N1-Cu1-N2	165.36(9)		
			2		
Cu1-N1	0.199 2(3)	Cu1-N3	0.199 5(3)	Cu1-O21	0.247 9(3)
Cu1-N2	0.209 1(3)	Cu1-N4	0.203 7(3)		
N1-Cu1-N3	172.04(14)	N3-Cu1-N4	86.39(12)	O21-Cu1-N2	103.73(10)
N1-Cu1-N2	94.37(12)	N4-Cu1-N2	157.69(12)	O21-Cu1-N4	98.44(10)
N1-Cu1-N4	88.35(12)	O21-Cu1-N1	88.63(11)		
N3-Cu1-N2	92.76(12)	O21-Cu1-N3	86.24(11)		

atoms and two Cl atoms, which is similar to [$CuCl_2$($C_{11}H_{21}N_3O$)][19]. The equatorial positions are occupied by three nitrogen atoms and one chloride atom in which the Cu-N and Cu-Cl bond lengths fall in the range of 0.198 1(2)~0.252 64(9) nm. One Cl atom occupies the axial position with the elongated Cu-Cl distance of 0.252 64(9) nm. The crystal packing is stabilized mainly by intermolecular N–H⋯Cl hydro-

Table 3 Hydrogen bond lengths and bond angles for complex 1 and 2

D–H···A	*d*(D-H) / nm	*d*(H···A) / nm	*d*(D···A) / nm	∠DHA / (°)
1				
N1a–H1Ca···Cl1	0.090	0.261	0.350 0(2)	170.0
N2–H2D···Cl2	0.090	0.245	0.334 1(2)	170.0
C9–H9···O1	0.093	0.250	0.333 0(4)	148.0
C14b–H14Bb···Cl2	0.096	0.277	0.370 5(3)	164.0
2				
N1a–H1Ba···N5	0.090	0.222	0.305 9(4)	155.0
N1–H1A···O23	0.090	0.221	0.310 2(4)	172.0
N3–H3A···O13	0.090	0.228	0.312 8(4)	157.0
N3–H3B···O11	0.090	0.223	0.308 4(4)	160.0

Symmetry codes: **1**: a: *x*, −1+*y*, *z*; b: −0.5+*x*, 2.5−*y*, 0.5+*z*; **2**: a: 1.5−*x*, −0.5−*y*, 1−*z*.

gen-bonding interactions.

2.3.2 Crystal structure of [Cu(4,4′-bipy)(amba)(ClO_4)] ClO_4 (**2**)

Unsymmetrical ellipsoid structural unit of complex **2** is given in Fig.3, together with the atom numbering scheme. Complex **2** contains a mononuclear cation [Cu(4,4′-bipy)(amba)(ClO_4)]$^+$ and one perchlorate anion. This complex is a centrosymmetric dimer, where each copper atom has a distorted square pyramidal geometry. The N1, N2, N3 and N4 are nearly coplanar, which constitute the base of the pyramid, whereas O21 occupies the apical position. The copper atom only deviates from the base plane 0.0163 0 nm. In the base plane, the four angles N1-Cu1-N2, N2-Cu1-N3, N3-Cu1-N4 and N4-Cu1-N1 are 94.36 (13)°, 92.77(13)°, 86.38(12)° and 88.37(12)°. The two pyridine rings are not on the same plane, the included angles of which and the benzene ring of the polyamine are 66.33° and 60.17°. The apical O21-Cu1 distance is 0.247 9 (3) nm, which is very near to the Cu-O bond length of 0.2498 nm reported from the literature [20]. The values of Cu-N (N1, N2, N3, and N4) distance range from 1.991 to 0.2091 nm, which is shorter compared with the distance reported from the literature[21]. Two molecular units join each other relying on the role of hydrogen-bond. Fig.4 reveals the connecting of the two complex molecules. In the figure, pyridine rings of the two molecules approximately locate in crisscross parallel position.

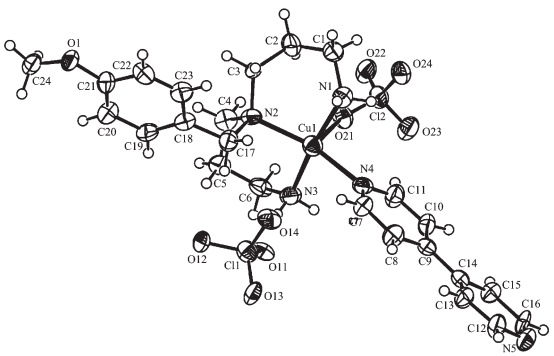

Fig.3 Unsymmetrical ellipsoid structural unit of complex **2** with 50% probability level

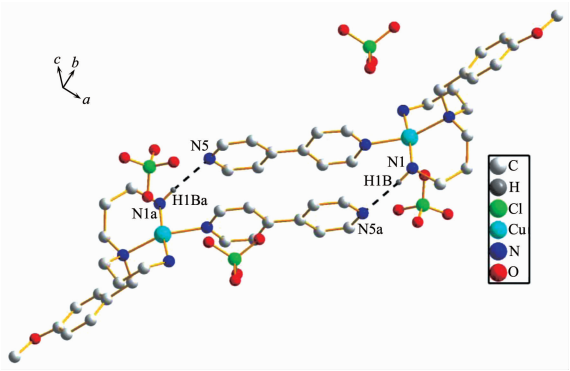

Symmetry codes: a: 1.5−*x*, −0.5−*y*, 1−*z*

Fig.4 Hydrogen bond interactions between two molecules of complex **2**

2.4 Absorption spectroscopic studies

Electronic absorption spectroscopy is one of the most useful methods for DNA-binding studies of metal complexes. The UV-Vis absorption spectrum of both metal complexes in double-distilled water is significantly perturbed by the addition of increasing concentrations of calf thymus DNA, which are shown in Fig. 5 and Fig.6. The spectrum both show a very strong absorption band at 225 nm and a relatively weaker

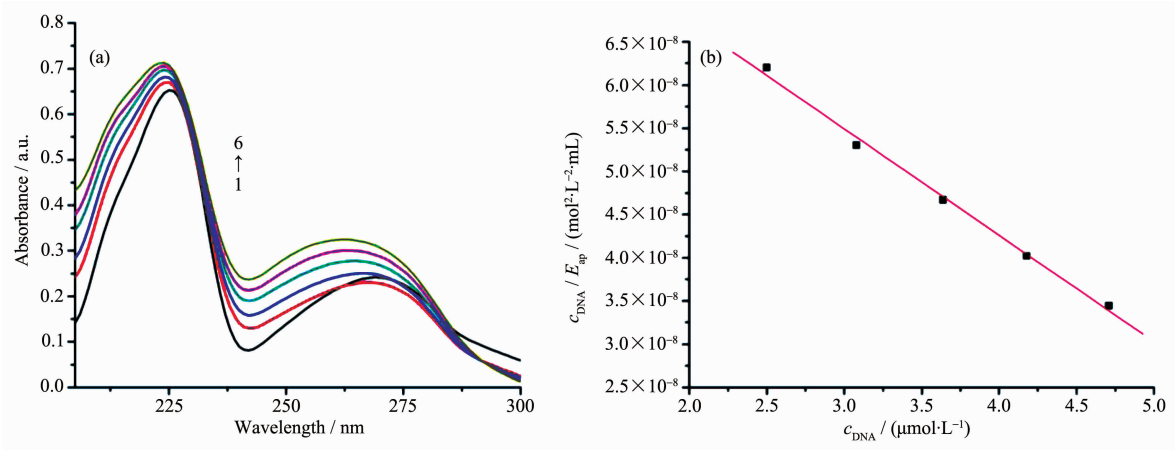

$c_{complex}$=50 μmol·L^{-1}, c_{DNA} / (μmol·L^{-1})=0 (1), 25.0 (2), 30.8 (3), 36.4 (4), 41.8 (5), 47.1 (6)

Fig.5　(a) Absorption spectra of complex **1** in double-distilled water upon addition of calf thymus DNA; (b) Plot of $c_{DNA}/(\varepsilon_a-\varepsilon_f)$ versus c_{DNA} for absorption titration of CT-DNA with complex **1**

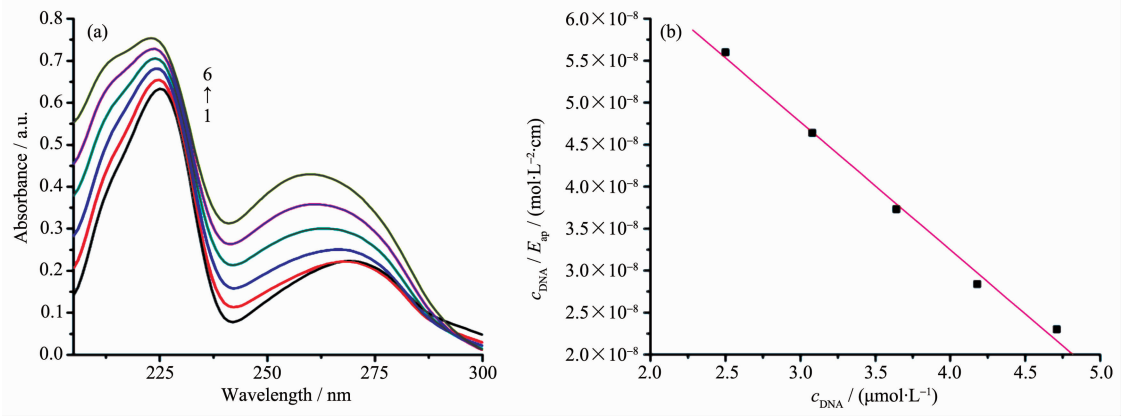

$c_{complex}$=50 μmol·L^{-1}, c_{DNA} / (μmol·L^{-1})=0 (1), 25.0 (2), 30.8 (3), 36.4 (4), 41.8 (5), 47.1 (6)

Fig.6　(a) Absorption spectra of complex **2** in double-distilled water upon addition of calf thymus DNA; (b) Plot of $c_{DNA}/(\varepsilon_a-\varepsilon_f)$ versus c_{DNA} for absorption titration of CT-DNA with complex **2**

absorption band at 271 nm, corresponding to π-π relative to aromatic groups and to metal-to-ligand charge transfer for the two complexes, and hyperchromicity was observed. With the increasing concentrations of CT-DNA, the maximum hyperchromism of 9.2% and 34.3% for complex **1**, meanwhile, the maximum hyperchromism of 19% and 92.4% for complex **2**. The blueshifts of 7 nm (for **1**) and 11 nm (for **2**) are observed at the secondary peak. The behaviors of the hyperchromism and blue-shift can be ascribed to the binding of the complex to the helix by an non-intercalative mode[22]. The extent of the hyperchromism is commonly consistent with the strength of intercalative interaction. In order to quantitatively investigate the binding strength, the intrinsic binding constant K_b was obtained by monitoring the changes in absorbance at 271 nm for the complex as increasing concentration of CT-DNA using Eq.(**1**). As are shown in Fig.5 and Fig. 6, the value of K_b was obtained from the ratio of slope to the intercept from the plot of $c_{DNA}/(\varepsilon_a-\varepsilon_f)$ versus c_{DNA}[23]. The calculated binding constants of **1** and **2** are 1.3×10^4 mol^{-1}·L and 1.7×10^4 mol^{-1}·L, respectively, which are much smaller than those reported for typical intercalators (e.g. EB-DNA, $K_b\sim10^6$ mol^{-1}·L)[24], while are comparable with some reported non-intercalators[25]. The low K_b values do favor electrostatic modes. What is more, the higher K_b value of **2** indicates the interaction of **2** with DNA is stronger than that of **1**.

2.5　Fluorescence spectroscopic studies

It is known metal complexes show no fluorescence in solution. Meanwhile, neither EB nor the solutions of the DNA has the fluorescent features[26]. But

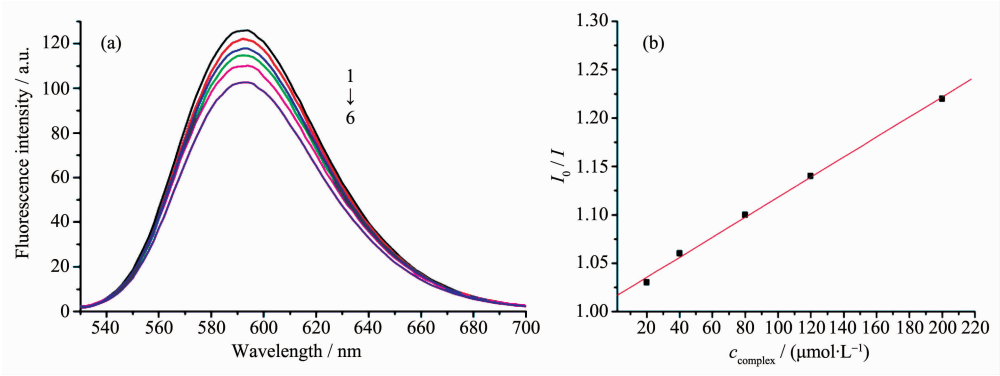

c_{EB}=4.0 μmol·L^{-1}, c_{DNA}=25.0 μmol·L^{-1}, $c_{complex\ 1}$ 1~6: 0, 20, 40, 80, 120, 200 μmol·L^{-1}, respectively; λ_{ex}=520 nm

Fig.7 (a) Emission spectra of EB bound to DNA in the absence (**1**) and presence (2~6) of complex **1** in double-distilled water, the figure shows the intensity changes on increasing the complex concentration; (b) Stern-Volmer quenching plots of EB bound to DNA by complex **1**

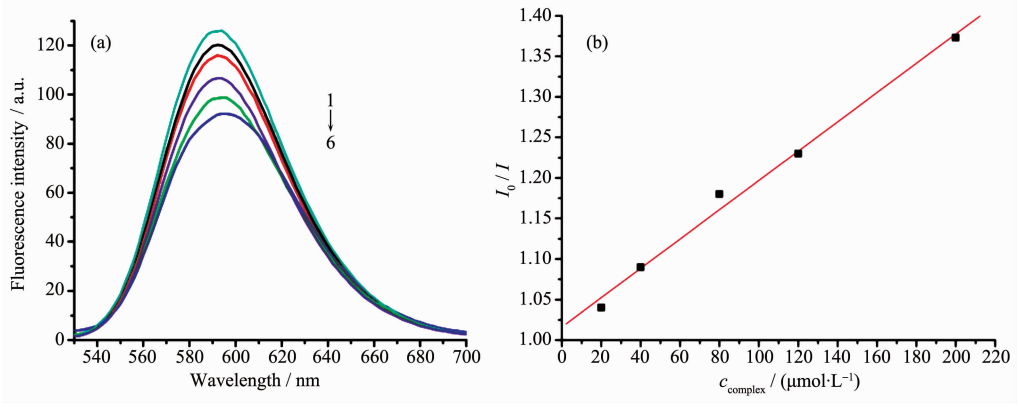

c_{EB}=4.0 μmol·L^{-1}, c_{DNA}=25.0 μmol·L^{-1}, $c_{complex\ 2}$ 1~6:0, 20, 40, 80, 120, 200 μmol·L^{-1}, respectively; λ_{ex}=520 nm

Fig.8 (a) Emission spectra of EB bound to DNA in the absence (**1**) and presence (2~6) of complex **2** in double-distilled water, the figure shows the intensity changes on increasing the complex concentration; (b) Stern-Volmer quenching plots of EB bound to DNA by complex **2**

the solutions of DNA with EB show very strongly fluorescence emission. If the complexes added to the EB-DNA system replace the bound EB, the emission emission will decrease. The emission spectra of EB bound to DNA in the absence and presence of the complexes are given in Fig.7 and Fig.8. From the figures, it can be seen clearly that the fluorescence intensity of the solutions are weaken after the complex has been added. The results confirm that the interaction activity of the complex binding to DNA enhance as its concentration increasing. The linear Stern-Volmer quenching constant of complexes **1** and **2** are 1.04×10^3 mol^{-1}·L and 1.81×10^3 mol^{-1}·L, respectively. Obviously, the two values are smaller than those of DNA-intercalative complexes[27], which suggests that the interaction of the two complexes with DNA replacing of the EB is not a intercalative mode, but a electrostatic mode. The results are consistent with absorption spectroscopic experiment.

2.6 Electrochemical studies

The cyclic voltammogram was employed to study the interaction of the redox active metal complexes in DMF to DNA at a scan of 100 mv·s^{-1}. The cyclic voltammetry (CV) curves of complexes **1** and **2** in the absence and presence of CT-DNA are shown in Fig.9 and Fig.10. In the absence of DNA, the cathodic peak potential (E_{pc}) and the anodic peak potential (E_{pa}) of the complex **1** are −0.64 V and −0.82 V, respectively. Half-wave potentials, $E_{1/2}$, taken as the average of E_{pa} and E_{pc}, is −0.73 V. The separation between the cathodic and anodic peak potential, ΔE is 0.18 V, which indicates that the electro chemical behavior of

the copper complex **1** is a quasi-reversible process[28]. When CT-DNA was added to the metal complex solution, which led in a remarkable loss in the cathodic and anodic peak current, owes to the interaction between the complex and DNA[29]. Meanwhile, the CV curve of complex **2** has a cathodic peak at −0.59 V and an anodic peak at −0.835 V. $E_{1/2}$ is −0.713 V, and ΔE is 0.245 V, which indicates a quasi-reversible process, a similar result as complex **1**.

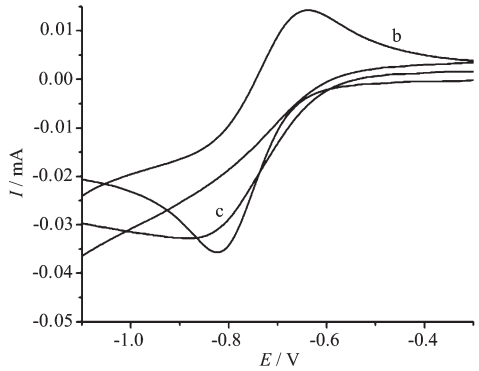

50 mmol·L^{-1} Tris-HCl/50 mmol·L^{-1} NaCl buffer solution (pH=7.2), $c_{\text{complex 1}}$=1×10^{-4} mol·L^{-1}

Fig.9　Cyclic voltammograms of complex **1** in the absence (b) and presence (c) of CT-DNA

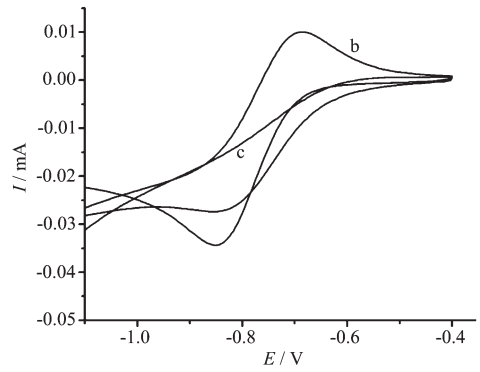

50 mmol·L^{-1} Tris-HCl/50 mmol·L^{-1} NaCl buffer solution (pH=7.2), $c_{\text{complex 2}}$=1×10^{-4} mol·L^{-1}

Fig.10　Cyclic voltammograms of complex **2** in the absence (b) and presence (c) of CT-DNA

2.7　Viscosity study

To further ascertain the interaction mode of the complex with DNA, a viscosity study was carried out. In general, non-intercalation like electrostatic bonding or grooving bonding mode will not affect lengthening of the DNA helix, leading to a minor change of DNA viscosity[30-31]. The results of the experiment indicate that the presence of the complex hardly exerts effect on DNA viscosity. As can be seen from Fig.11, both of the viscosity of DNA faintly increase with increasing complexes concentration, suggesting that the binging modes of the two complexes interact with DNA may belong to electrostatic mode[30-31].

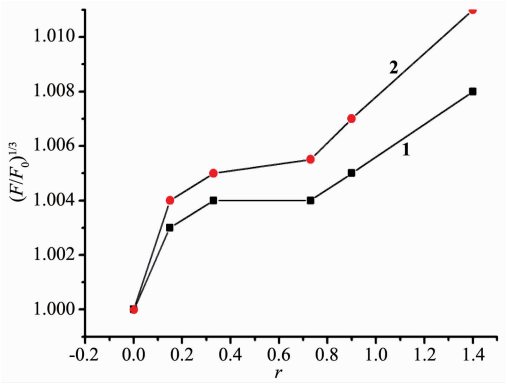

CT-DNA at 23 (±0.1) ℃, c_{DNA}=100 μmol·L^{-1}, r=c_{complex}/c_{DNA}

Fig.11　Effects of increasing amounts of complex **1** and **2** on the relative viscosities

2.8　DNA cleavage

In order to evaluate the function of the two complexes to incise DNA, the cleavage reaction of supercoiled pBR322 DNA was monitored by agarose gel electrophoresis. All experiments were performed in TAE buffer solution (pH 7.2). After reaction for 4 h, the supercoiled form opens to form an open circular and finally to a linear form (linear DNA). As a result, the DNA gets degraded into small pieces which cannot be distinguished in our assay. The cleavage products were subjected to gel electrophoretic separation and the gels analysed after ethidium bromide staining.

As is shown in Fig.12, both the two complexes can transform the supercoiled (SC) to nicked circular (NC) DNA form, and the concentration of the complexes has no distinct effect on the cleavage activity. Fig.13 shows the time dependence of the cleavage reactions of DNA with the complexes after incubation. With increasing incubation time, the cleavage of DNA did not change obviously. Comparing with the other copper complexes in the literature[32], the two complexes have an efficient cleavage of DNA.

In order to further clarify the DNA cleavage mechanism, cleavage trials were carried out in the presence of typical scavengers for singlet oxygen

(NaN_3, 3 mmol·L^{-1}), for superoxide (KI, 3 mmol·L^{-1}), and for hydroxyl radical (DMSO, 3 mmol·L^{-1} and EtOH, 3 mmol·L^{-1}). As can be seen in Fig.14, no obvious change of DNA cleavage activity of the complexes is

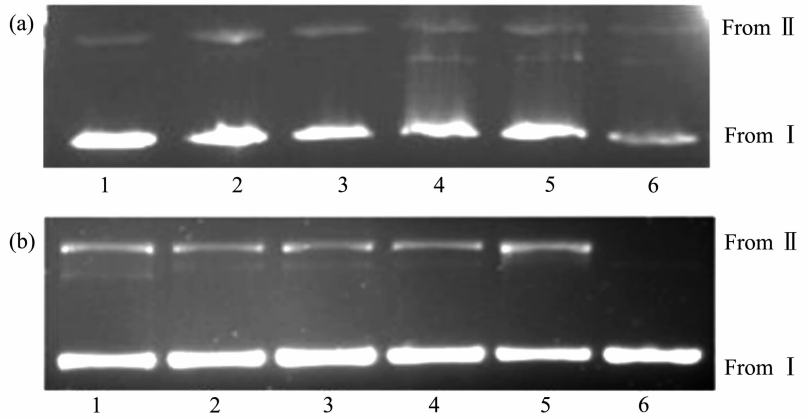

Complexes were incubated in 50 mmol·L^{-1} Tris-HCl/NaCl buffer at 37 ℃. Lane 1~5, DNA+complex (25, 50, 100, 150, 200 μmol·L^{-1}), respectively; Lane 6, DNA control; a for **1** and b for **2**

Fig.12 Agarose gel electrophoresis of pBR322 plasmid DNA in the presence of different concentrations

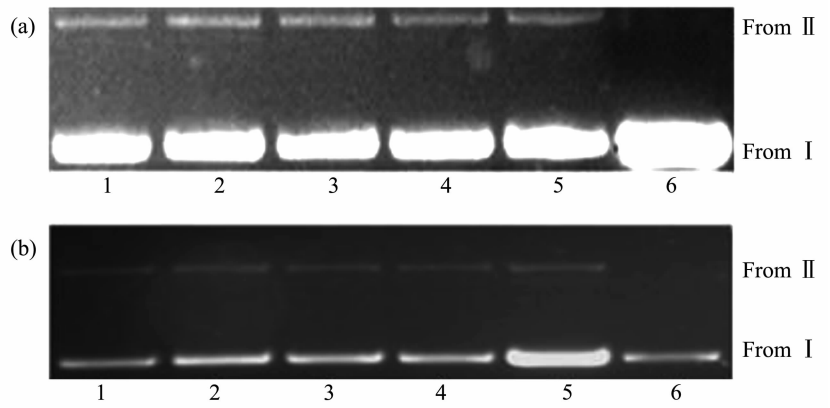

c(DNA)=0.5 μg·μL^{-1}, with the complexes after incubation in 50 m mol·L^{-1} Tris–HCl/NaCl buffer (pH=7.2) at 37 ℃: Lane 1~5, DNA+complex (100 μmol·L^{-1}) for 1 h, 2 h, 3 h, 4 h, 5 h, Lane 6, DNA control; a for **1** and b for **2**

Fig.13 Time dependence of the cleavage of pBR322 DNA

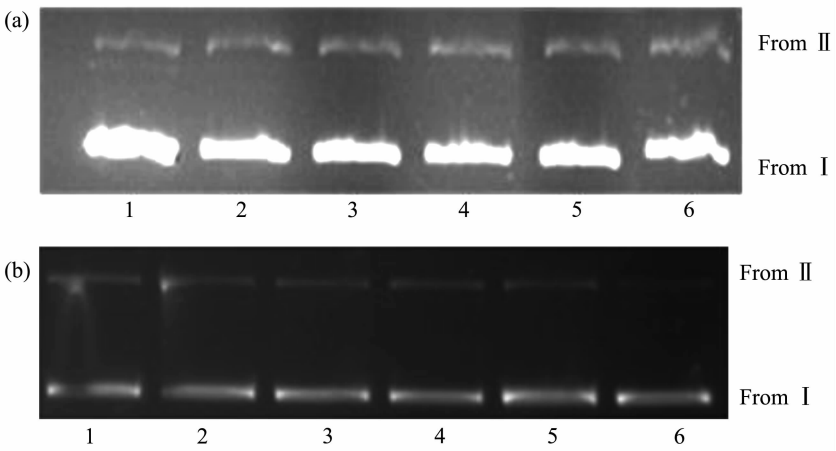

c_{DNA}=0.5 μg·μL^{-1}, by the complexes at different scavenging agents in 50 mmol·L^{-1} Tris-HCl/NaCl buffer (pH=7.2) and 37 ℃ for 4 h: Lane 2~5, DNA+complex (100 μmol·L^{-1})+3 mmol·L^{-1} NaN_3; KI; DMSO; EtOH. Lane 1, DNA+complex (100 μmol·L^{-1}); Lane 6, DNA control; a for **1** and b for **2**

Fig.14 Gel electrophoresis diagram showing the cleavage of pBR322 DNA

observed. That is, DNA cleavage promoted by the two complexes might not occur by an oxidative pathway but rather by a hydrolytic pathway.

3 Conclusions

In conclusion, two polyamine copper complexes were prepared and structurally characterized. In the comparative DNA binding studies, the binding modes of the two complexes interacting with DNA were confirmed to be electrostatic modes, and complex **2** binding capacity was slight higher than **1**. The interaction occurrence is supported by the following three findings: (i) the binding constants (K_b) values are 1.3×10^4 $mol^{-1}\cdot L$ for complex **1** and 1.7×10^4 $mol^{-1}\cdot L$ for **2**; (ii) the linear Stern-Volmer quenching constants of complexes **1** and **2** are 1.04×10^3 $mol^{-1}\cdot L$ and 1.81×10^3 $mol^{-1}\cdot L$, respectively; (iii) the DNA viscosity of the two complexes faintly increase with increasing complexes concentration, also suggesting that the binging modes may be not intercalative modes but electrostatic modes.

Finally, the two complexes show an efficient cleavage activity toward supercoiled DNA (pBR322 DNA) in the DNA cleavage study. We propose the DNA cleavage promoted by the complexes occur via a hydrolytic pathway.

References:

[1] (a)Leininger S, Olenyuk B, Stang P J. *Chem. Rev.*, **2000**,**100**:853-908
(b)Brammer L. *Chem. Soc. Rev.*, **2004**,**33**:476-489
(c)James S L. *Chem. Soc. Rev.*, **2003**,**32**:276-288
(d)Kitagawa S, Uemura K. *Chem. Soc. Rev.*, **2005**,**34**:109-119

[2] Tadokoro M, Yasuzuka S, Nakamura M, et al. *Angew. Chem. Int. Ed.*, **2006**,**45**:5144-5147

[3] Kirillov A M, Karabach Y Y, Haukka M, et al. *Inorg. Chem.*, **2008**,**47**:162-175

[4] (a)Wang H, Li M X, Shao M, et al. *Polyhedron*, **2007**,**26**:5171-5176
(b)Kong L Y, Lu X H, Huang Y Q, et al. *J. Solid State Chem.*, **2007**,**180**:331-338

[5] Kong L Y, Zhu H F, Okamuro T, et al. *J. Inorg. Biochem.*, **2006**,**100**:1272-1279

[6] (a)Qi Z P, Ba Z S, Yuan Q, et al. *Polyhedron*, **2008**,**27**:2672-2678
(b)Lu H J, Fan Y T, Gao J, et al. *Synth. React. Inorg. Metal-Org. Nano-Metal Chem.*, **2005**,**35**:305-309

[7] (a)Kong L Y, Zhang Z H, Zhu H F, et al. *Angew. Chem. Int. Ed.*, **2005**,**44**:4352-4355
(b)Kong L Y, Zhu H F, Huang Y Q, et al. *Inorg. Chem.*, **2006**,**45**:8098-8107

[8] Carla B, Bencini A, Bianchi A, et al. *J. Org. Chem.*, **2008**,**73**:8286-8295

[9] Nagamani D, Ganesh K N. *Org. Lett.*, **2001**,**3**(1):103-106

[10](a)Macias B, Villa M V, Sanz F, et al. *J. Inorg. Biochem.*, **2005**,**99**:1441-1448
(b)Vaidyanathan V G, Nair B U. *J. Inorg. Biochem.*, **2003**,**93**(3-4):271-276
(c)Tan L F, Chao H, Liu Y J, et al. *Inorg. Chim. Acta*, **2005**,**358**:2191-2198

[11](a)Vaidyanathan V G, Nair B U. *J. Inorg. Biochem.*, **2002**,**91**:405-412
(b)Cejudo R, Alzuet G, Gonzalez-Alvarez M, et al. *J. Inorg. Biochem.*, **2006**,**100**:70-79
(c)Zhang Q L, Liu J G, Chao H, et al. *J. Inorg. Biochem.*, **2001**,**83**:49-55

[12](a)Sreedhara A, Frued J D, Cowan J A. *J. Am. Chem. Soc.*, **2000**,**122**:8814-8824
(b)Mancin F, Scrimin P, Tecilla P, et al. *Chem. Commun.*, **2005**,**20**:2540-2548

[13](a)Wang X Y, Zhang J, Li K, et al. *Bioorg. Med. Chem.*, **2006**,**14**:6745-6751
(b)Ademir N, Herna′n T, Rosmari H, et al. *Chem. Commun.*, **2001**,**4**(8):388-391

[14](a)Koike T, Takamura M, Kimura E. *J. Am. Chem. Soc.*, **1994**,**116**:8443-8449.
(b)Koike T, Kajitani S, Nakamura I, et al. *J. Am. Chem. Soc.*, **1995**,**117**:1210-1219
(c)Kimura E, Nakamura I, Koike T, et al. *J. Am. Chem. Soc.*, **1994**,**116**:4764-4771
(d)Kimura E, Shionoya M, Hoshino A, et al. *J. Am. Chem. Soc.*, **1992**,**114**:10134-10137
(e)Koike T, Kimura E. *J. Am. Chem. Soc.*, **1991**,**113**:8935-8941
(f)Kimura E, Shiota T, Koike T, et al. *J. Am. Chem. Soc.*, **1990**,**112**:5805-5811

[15]Xia J, Xu Y, Tang W X. *Inorg. Chem.*, **2001**,**40**(10):2394-2401

[16]Hu H, Chen Y F, Zhou H. *Trans. Met. Chem.*, **2005**,**36**:395-402

[17]*SMART and SAINT, Area Detector Control and Integration Software*, Simens Analytical X-Systems, Inc., Madison, WI,

USA, **1996**.

[18]Sheldrick G M. *SHELXTL V*5.1 *Software Reference Manual*. Bruker AXS Inc., Madison, **1997**.

[19]Wang P, Wang X H, Liu H, et al. *Acta Cryst.*, **2007**,**E63**: m3001/1-8

[20]Hu D, Chen L, Pan Z Q, et al. *J. Coord. Chem.*, **2008**,**61** (12):1973-1982

[21]Sun W W, Li S R, Zhou H, et al. *Z. Anorg. Allg. Chem.*, **2009**,**635**:1-6

[22]Tang S P, Hou L, Mao Z W, et al. *Polyhedron*, **2009**,**28**:586-592

[23]Pyle A M, Rehmann J P, Kumar C V. *J. Am. Chem. Soc.*, **1989**,**111**:3051-3058

[24]Baldini M, Belicchi-Ferrari M, Bisceglie F. *Inorg. Chem.*, **2004**,**43**:7170-7179

[25]Chen J W, Wang X Y, Shao Y, et al. *Inorg. Chem.*, **2007**, **46**:3306-3312

[26]Meyer-Almes F J, Porschke D. *Biochem.*, **1993**,**32**:4246-4253

[27]Tian J L, Feng L, Gu W. *J. Inorg. Biochem.*, **2007**,**101**:196-202

[28]Zhang J A, Pan M, Yang R, et al. *Polyhedron*, **2010**,**29**:581-589

[29]Aslanoglu M. *Anal. Sci.*, **2006**,**22**:439-443

[30]Liu J G, Ye B H, Li H, et al. *J. Inorg. Biochem.*, **1999**,**76**: 265-271

[31]Sankar J, Rath H, Prabhuraja V, et al. *Chem. Eur. J.*, **2007**, **13**(1):105-114

[32]Li D D, Tian J L, Gu W, et al. *Eur. J. Inorg. Chem.*, **2009**: 5036-5045